Journal of Molecular Catalysis A: Chemical 355 (2012) 192–200

Contents lists available at SciVerse ScienceDirect

Journal of Molecular Catalysis A: Chemical

journal homepage: www.elsevier.com/locate/molcata

Catalytic oxidation of polyphenol trihydroxybenzene by copper(II) β-alanylsulfadiazine complex

Ahmed I. Hanafy[a,*,1], Zeinhom M. El-Bahy[a,1], Ahmed A. El-Henawy[b], Abeer A. Faheim[a,1]

[a] Chemistry Department, Faculty of Science, Taif University, Taif, Saudi Arabia
[b] Al-Azhar University, Faculty of Science, Cairo, Egypt

ARTICLE INFO

Article history:
Received 12 August 2011
Received in revised form 7 December 2011
Accepted 9 December 2011
Available online 17 December 2011

Keywords:
Sulfadiazine
β-Alanine
Oxidation
Trihydroxybenzene

ABSTRACT

The copper(II) complex of sulfadiazine with β-alanine amino acid was synthesized and characterized using different tools such as IR, UV/Vis, ^{1}H NMR, elemental analysis, thermal analysis, TEM and EPR spectroscopy. The mode of binding of the metal shows that, the copper binds with the ligand through nitrogen atom of the amino group and carbonyl oxygen atom. The transmission electron microscope (TEM) demonstrated that the average particle size of the copper complex is found to be in the range of 35–40 nm. The complex, [CuL(OH)$_2$] has been used as an effective catalyst for homogenous oxidation of polyphenol 1,2,3-trihydroxybenzene in the presence of the green oxidant H_2O_2 to produce a first-order rate constant $k_{cat} = 0.0043\ s^{-1}$. The catalysis shows a catalytic proficiency of 1.7×10^3 times compared to the uncatalyzed oxidation of THB under the same reaction conditions. The oxidation reaction is inhibited by kojic acid with $IC_{50} = 65\ \mu M$.

1. Introduction

The oxidation of organic substrates with molecular oxygen under mild conditions is of great interest for industrial and synthetic processes, especially from economical and environmental points of view [1,2]. Although the reaction of organic compounds with dioxygen is thermodynamically favored it is kinetically hindered due to the triplet ground state of O_2. The synthesis and investigation of functional model complexes for metalloenzymes with oxidase or oxygenase activity is therefore of great interest for the development of new and efficient catalysts for oxidation reactions.

Catechol oxidase, tyrosinase, and polyphenol oxidases are analogous metalloenzymes which oxidize phenolic compounds to the corresponding quinones in the presence of oxygen. This kind of reaction is of great importance in medical diagnosis for the determination of the hormonally active catecholamines adrenaline, noradrenaline and dopa [3]. There have been great efforts to synthesize model complexes as functional or structural models for catechol oxidases or related copper containing enzymes [4–9].

Transition metal complexes have been widely studied in the area of bio-inorganic, bio-organic, and catalytic chemistry [10–13]. Copper complexes are interesting compounds in the field of oxidation catalysis as copper-containing oxidases. These biomimetic chemical systems may be better accessible, more stable and more catalytically versatile than enzymes, thus may have wider applications and provide chemical insight into the mechanisms of enzymes [14–16].

Sulfadiazine compound has been chosen in this study due to its relatively small molecular weight, its biological activity and medicinal uses. We have prepared a new simple and an environment friendly copper(II) complex derived from the antibacterial sulfadiazine with β-alanine amino acid. This complex was characterized and used as biomimetic of a copper-containing oxidase in the oxidation of trihydroxybenzene.

2. Experimental

2.1. Materials

Sulfadiazine, β-alanine, N,N′-dicyclohexylurea, 1,2,3-trihydroxybenzene and Fmoc (9*H*-fluoren-9-ylmethoxycarbonyl) were purchased from Sigma–Aldrich. Kojic acid and copper chloride were purchased from Merck Company.

2.2. Synthesis of 3-amino-N-[4-(pyrimidine-2-ylsulfamoyl)-phenyl]-propionamide (β-alanylsulfadiazine)

A mixture of sulfadiazine (0.01 mol) and Fmoc-β-alanine (0.01 mol) was dissolved in ~30 ml tetrahydrofuran. The mixture was cooled to 0 °C and then (2.06 g; 0.01 mol)

* Corresponding author. Taif University, Faculty of Science, Taif, Saudi Arabia. Tel.: +966 28322143; fax: +966 28322143.
E-mail address: ahmedih@yahoo.com (A.I. Hanafy).
[1] Permanent address: Al-Azhar University, Faculty of Science, Cairo, Egypt.

1381-1169/$ – see front matter © 2011 Elsevier B.V. All rights reserved.
doi:10.1016/j.molcata.2011.12.016

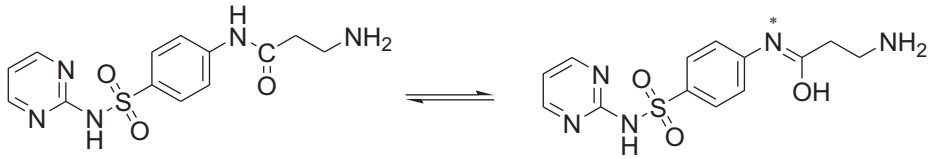

Structure 1. Keto–enol tautomeric forms of βAS ligand.

N,N′-dicyclohexylcarbodiimide (DCCD) dissolved in ~10 ml tetrahydrofuran was added. The reaction mixture was stirred for 3–5 h at 0 °C and allowed to stand for 24 h at room temperature. A few drops of acetic acid and water were added, then the precipitate of N,N′-dicyclohexylurea was filtered off. The filtrate was concentrated in vacuo to dryness. The residual material was recrystallized from ethanol–water, and obtained in 80% yield, Structure 1. The compound was chromatographically homogenous when developed with iodine solution-benzidine and gave a negative ninhydrin test.

2.3. Synthesis of Cu^{II}—βAS complex

Copper(II) chloride (0.1 mol) was dissolved in ~40 ml absolute ethanol, then added to 0.1 mol of the prepared ligand β-alanylsulfadiazine (βAS) dissolved in ~40 ml absolute ethanol. The mixture was heated under reflux for ~2 h. The bluish precipitate was formed, filtered off and finally washed with hot ethanol several times.

2.4. Physical methods

Carbon, hydrogen and nitrogen contents were determined at the Microanalytical Unit, Cairo University, Egypt. IR spectra of the ligand and its solid complexes were measured in KBr on a Mattson 5000 FTIR spectrometer. All electronic spectra and kinetic measurement were performed using a Varian Cary 4 Bio UV/Vis spectrophotometer. The ^{1}H NMR spectrum of the ligand was recorded on JEOL-90Q Fourier Transform (200 MHz) spectrometers in [d_6] DMSO. Thermal analysis measurements (TGA, DTA) were recorded on a Shimadzu thermo-gravimetric analyzer model TGA-50H, using 20 mg samples. The flow rate of nitrogen gas and heating rate were 20 cm^3 min^{-1} and 10 °C min^{-1} respectively. ESR spectra were obtained on a Bruker EMX spectrometer working in the X-band (9.78 GHz) with 100 kHz modulation frequency. The microwave power and modulation amplitudes were set at 1 mW. The mass spectrum of the ligand was recorded on a Shimadzu GC-S-QP 1000 EX spectrometer using a direct inlet system. Thermal analysis, ESR and mass spectroscopy were recorded at Cairo University, Egypt. The magnetic susceptibility measurements for the complexes were determined using Gouy balance with Hg[$Co(NCS)_4$] as a calibrant at room temperature. Transmission electron microscope (TEM) micrographs were measured using JEOL JEM-1010 transmission electron microscope, at an accelerating voltage of 60 kV. Suspensions of the samples were put on carbon foil with a micro grid. TEM images were observed with minimum electron irradiation to prevent damage to the sample structure.

2.5. Molecular modeling methods

2.5.1. Conformational analysis

Initial molecular structures of the ligands were built using the HyperChem program 7.5. The conformational analysis has been performed by use of MM+ (calculations in vacuo, bond dipole option for electrostatics, Polake Ribiere algorithm, and RMS gradient of 0.01 kcal/mol). Minimum energy for compounds was performed by a semi-empirical method PM3 (as implemented in HyperChem 7.5). The resulting conformations were confirmed as minima by vibrational analysis.

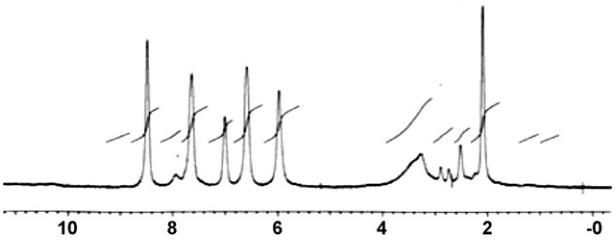

Fig. 1. ^{1}H NMR of β-alanylsulfadiazine in d_6-DMSO.

2.6. Kinetic reactions for trihydroxybenzene (THB) oxidation

The catalytic activity of the Cu^{II}—βAS complex toward the homogeneous oxidation of trihydroxybenzene (THB) in ethanol solution at 25 °C was determined by measuring the initial rate of (THB) oxidation. The increase of the absorption at 420 nm (ε = 4583 M^{-1} cm^{-1}) due to the oxidation product [17] with time was obtained on a Varian Cary 3E spectrophotometer. A plot of the formation of the product with respect to time gives the initial rate. To study the effect of the catalyst concentration on the rate of the reaction, various amounts of the copper(II) complex (10–300 μM) have been used with 200 μM H_2O_2 for oxidation of 1.0 mM THB at 25 °C. In the same time 30 μM of the catalyst has been used in the oxidation of different concentrations of the substrate (5–80 mM) in the presence of 200 μM H_2O_2 to study the effect of THB concentration on the reaction. The rate laws were determined and rate constants obtained. The dependence of H_2O_2 on THB oxidation by 30 μM Cu^{II}—βAS was determined by measuring the oxidation rate at different concentrations of hydrogen peroxide (25–400 μM) in the presence of 1.0 mM THB in ethanol at 25 °C. The auto-oxidation rate of THB was determined under the same conditions in the absence of Cu^{II}—βAS. Inhibitions were carried out in a similar fashion as the kinetic measurements using 30 μM Cu^{II}—βAS in the presence of 200 μM H_2O_2 and different amounts of kojic acid.

3. Results and discussion

3.1. IR and ^{1}H NMR spectra

The organic ligand (β-alanylsulfadiazine) has been prepared using (Fmoc) as a protective group which is generally removed from the N terminus of a peptide chain by acidolysis using trifluoroacetic acid (TFA) [18]. The IR spectrum of the 3-amino-N-[4-(pyrimidine-2-ylsulfamoyl)-phenyl]-propionamide(β-alanylsulfadiazine) shows bands at 3425, 3358 and 3259 cm^{-1} assigned to νNH and νNH_2, respectively. The ligand also shows bands at 1649, 1586, 1494 and 1441 cm^{-1} assigned to νC=O, νC=N, β-NH_2 and ν(O=S=O), respectively [19,20]. ^{1}H NMR spectrum of β-alanylsulfadiazine in dimethyl-sulfoxide-d_6 (Fig. 1) exhibited signals at δ = 2.7 (d, 2H, CH_2—C**H**$_2$$CH_2NH_2$), 3.2 (b, 2H, CH_2—C**H**$_2$$NH_2$), 5.9 (s, 1H, NH—$SO_2$N**H**), 6.5–7.4 (m, aromatic

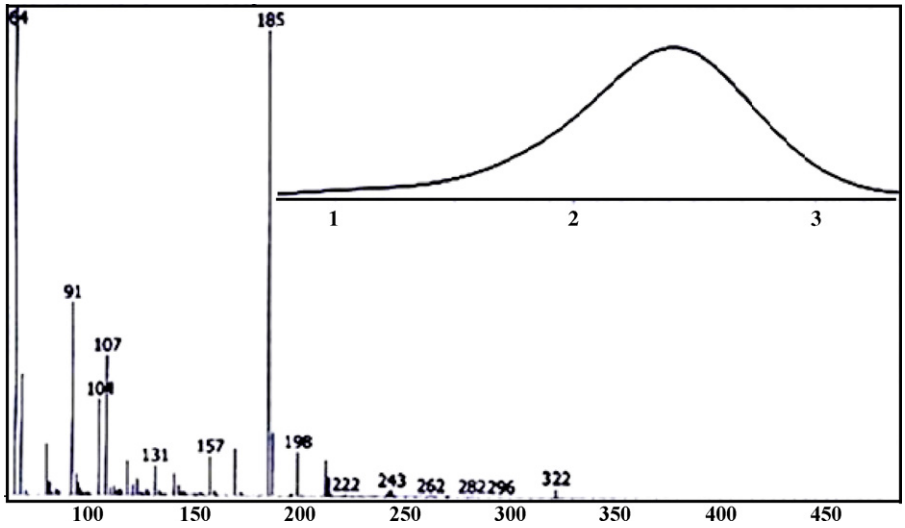

Fig. 2. Mass spectrum of the organic ligand βAS. Inset indicates the purity of the ligand βAS.

protons), 7.8 (b, 2H, NH_2), 8.4 (s, 1H, NH—N**H**CO). All these data together with the molecular weight determined from mass spectrometry [Fig. 2 and Scheme 1 (m/z = 322)] suggest the structure of the βAS ligand as shown in Structure 1.

By comparing the IR spectral data of the ligand with that of the Cu(II) complex, it is found that the copper(II) binds to βAS through the nitrogen atom of NH_2 and carbonyl oxygen atom. This suggestion was supported by shifting in carbonyl band to lower wavenumber in the complex spectrum (1610 cm^{-1}) with a decrease in its intensity. Moreover, this is also supported by shifting in νNH_2 bands to higher wavelength (3953 and 3357 cm^{-1}). The bands attributed to νNH and ν(O═S═O) remain at the same position as in the ligand spectrum, indicating no participation of NH or SO_2 functional groups in the coordination. The coordination of NH_2 nitrogen atom is also consistent with the presence of a new band at 464 cm^{-1} due to νCu—N. The IR spectrum shows a broad band observed at

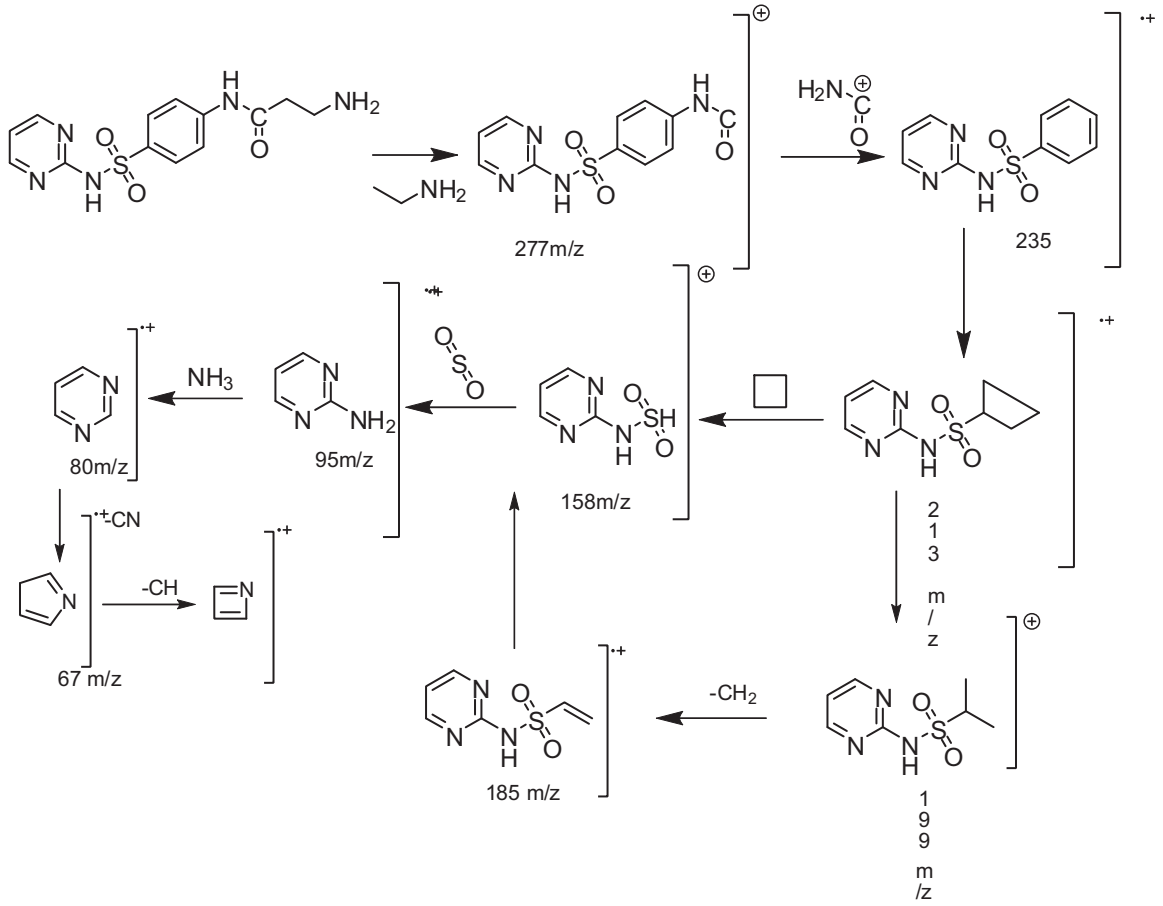

Scheme 1. Mass fragmentation pattern of βAS.

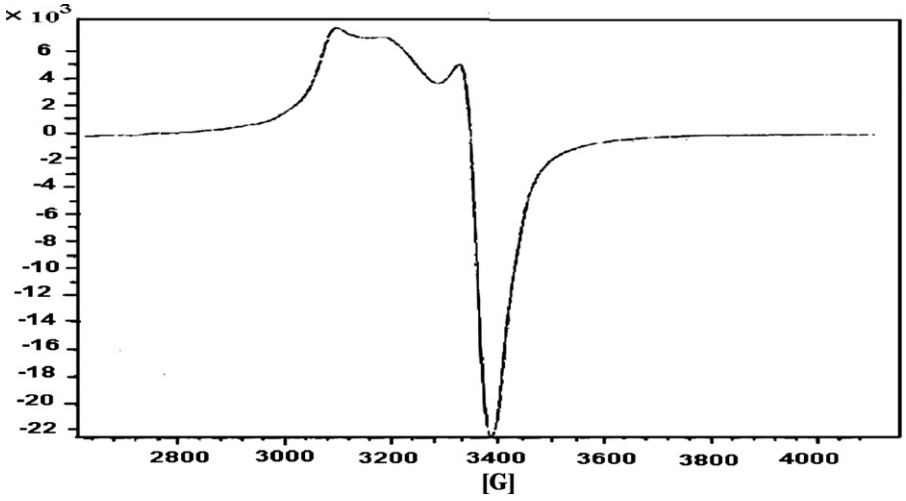

Fig. 3. EPR spectrum of Cu^{II}—βAS complex.

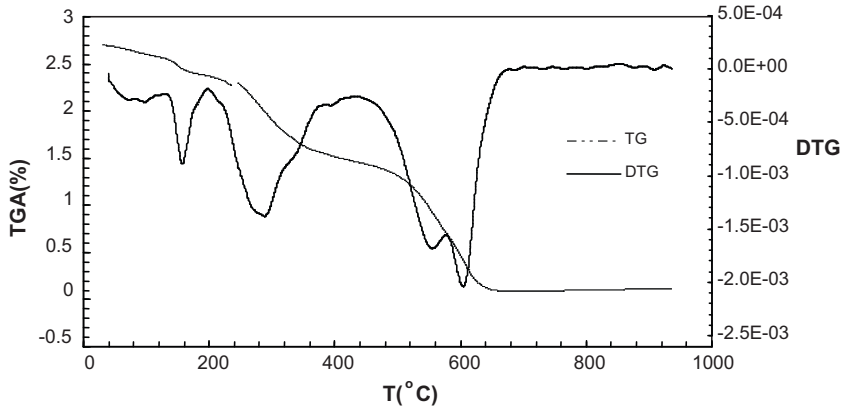

Fig. 4. TGA and DTG of the copper complex Cu^{II}—βAS.

~3420 cm^{-1} assigned to νOH stretching vibration. The proposed structure is confirmed by the presence of new band at 555 cm^{-1} attributed to Cu—O.

3.2. Electronic spectral data

The magnetic moment (1.8 BM) of the Cu(II) complex Cu^{II}—βAS at room temperature corresponds to one unpaired electron [21]. The electronic spectrum of Cu^{II}—βAS complex recorded in ethanol reveals an absorption band at 495 nm. This band can be attributed to d–d transition ($^2B_{1g} \rightarrow {}^2A_{1g}$), which support square-planar geometry around the metal ion [22]. The bands at 280 and 370 nm can be assigned to a CT band from filled orbitals Cu(II) to the anti-bonding π^* orbitals of the ligand [23].

The EPR spectrum of the Cu^{II}—βAS complex was recorded as a polycrystalline sample at room temperature. The spectrum of the complex exhibits a single anisotropic broad signal. The analysis of the spectrum (Fig. 3) gives the $g_{||} = 2.1212$ and $g_{\perp} = 2.0811$. These values indicate that the ground state of Cu(II) is predominately d_{x2-y2}, which supports a square planar structure [24,25]. The observed $g_{||}$ value for Cu^{II}—βAS is less than 2.3, thus, indicating that the bonds between the organic ligand and copper ion have a covalent character more than the ionic one. According to Hathaway and Billing [26,27], the $G = (g_{||} - 2)/(g_{\perp} - 2)$, which measures the exchange interaction between the copper centers in a polycrystalline solid has been calculated and found to be less than 4.0. This value indicates to a considerable exchange interaction in solid complex. The elemental analysis calcd. (%) for Cu^{II}—βAS: C, 37.40; H, 4.07; N, 16.80; Cu, 15.20. Found: C, 38.01; H, 3.93; N, 15.97; Cu, 15.11, in addition to the IR, electronic and EPR spectral data suggest that the structure of the Cu^{II}—βAS complex is [$CuL(OH)_2$], where L = βAS, as shown in Structure 2.

3.3. Thermal analysis

The TGA thermogram confirms the amount of solvent inside and/or outside the coordination sphere and gives some information about the stability of this compound. The thermogram of Cu^{II}—βAS (Fig. 4) shows three stages of mass loss over the temperature range of 25–800 °C. The first stage at 140 °C corresponds to removal of one water molecule inside the coordination sphere with weight loss (calcd. = 4.3%, found = 5.0%). The second peak in the temperature range of 240–350 °C corresponds to removal of $CH_3CH_2NH_2$, SO_2 and CO_2 molecules with weight loss (calcd. = 36.5%, found = 37.0%). The third inflection point

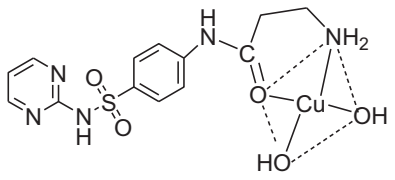

Structure 2. Chemical structure of Cu^{II}—βAS complex.

Table 1
Thermodynamic parameters for Cu^{II}—βAS complex.

Decomposition temperature (K)	E (kJ mol^{-1})	ΔS (J K^{-1} mol^{-1})	ΔH (kJ mol^{-1})	ΔG (kJ mol^{-1})
420–437	17.9	−290	14.4	136.2
510–594	17.0	−321	12.4	189.6
781–897	15.3	−345	8.1	307.9

corresponds to $C_6H_5NH_2$ (aniline) and $C_4H_5N_3$ (pyridine-2-amine) with weight loss (calcd. = 44.9%, found = 45%).

The thermodynamic activation parameters of the decomposition process were evaluated using the well known Coats–Redfern equation [28] in the form:

$$\ln\left[\frac{-\ln(1-\alpha)}{T^2}\right] = -\frac{E}{RT} + \ln\frac{AR}{\beta E} \quad (1)$$

where α is the fraction of decomposition, R is the universal gas constant, E is the activation energy, A is constant and β is the heating rate. Therefore, plotting $\ln[-\ln(1-\alpha)/T^2]$ against $1/T$ according to Eq. (1) gives a straight line whose slope is directly proportional to the activation energy ($-E/R$). The activation entropy ΔS, the activation enthalpy ΔH, and the free energy (Gibbs function ΔG) were calculated (Table 1) using the following equations [29]:

$$\Delta S = 2.303\left(\log\frac{Ah}{kT}\right)R \quad (2)$$

$$\Delta H = E - RT \quad (3)$$

$$\Delta G = \Delta H - T\Delta S \quad (4)$$

where k and h are Boltzmann's and Planck's constants respectively, T is the temperature involved in the calculation and selected as the peak temperature of DTGA. The entropy ΔS gives information about the degree of disorder of the system, the enthalpy ΔH gives information about the total thermal motion and Gibbs or free energy gives information about the stability of the system.

The Cu^{II}—βAS complex was examined via transmission electron microscope (TEM). Fig. 5 shows that the average particle size of the copper(II) complex is in the range of 35–40 nm diameters. The simplicity in the preparation of this Cu(II) complex and its high activity suggest potential application of this synthetic model as oxidative catalyst for further investigation of Cu-centered oxidation and oxygenation chemistry and medical diagnosis for determination of some hormones [3]. Based on the concept that the attachment of nanoparticles onto electrodes dramatically enhances the conductivity and electron transfer from the redox analytes [30], this complex can be used as electrochemical sensor [31] in bioelectrocatalytic reactions.

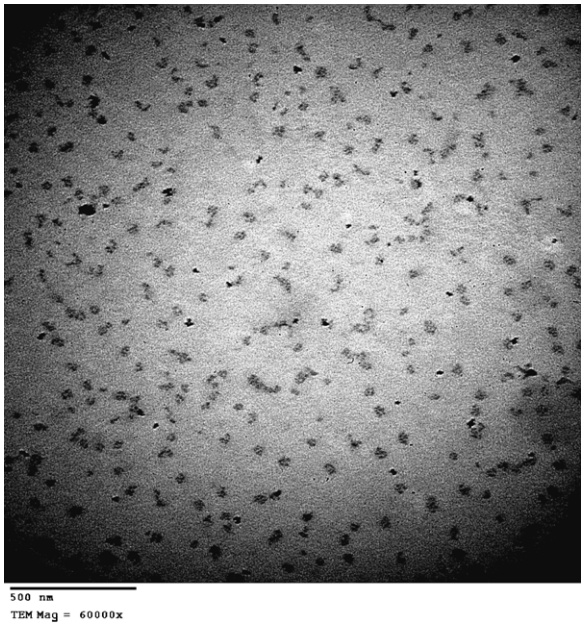

Fig. 5. TEM images of the Cu^{II}—βAS complex.

Table 2
Calculated energies of keto–enol tautomeric forms of βAS ligand and Cu^{II}—βAS complex.

Complex	Enol form	Keto form	Method PM3
−179.54	−4.407	−7.68	Heat of formation (kcal/mol)
−4204.91	−3789.97	−3793.804	Total energy (kcal/mol)
−4244.63	−3817.58	−3820.86	Binding energy (kcal/mol)
−9.00	−9.63	−9.68	HOMO (eV)
−9.16	−9.44	−9.65	LUMO (eV)
5.92	2.61	3.77	Dipole (Deby)

$$Cu^{II}\text{—}\beta AS + S \underset{k_{-1}}{\overset{k_1}{\rightleftharpoons}} (Cu^{II}\text{—}\beta AS) - S \xrightarrow{k_{cat}} Cu^{II}\text{—}\beta AS + \text{Prod.} \quad (5)$$

$$\text{rate} = \frac{k_{cat}[Cu^{II}\text{—}\beta AS][S]}{K' + [S]} \quad (6)$$

$$\frac{[THB]}{V_o} = \frac{1 + (K'_{H_2O_2}/[H_2O_2])}{V_{max}}[THB] + \frac{K'_{THB}}{V_{max}}\left(1 + \frac{K_{i(H_2O_2)}}{[H_2O_2]}\right) \quad (7)$$

3.4. Molecular modeling

In trying to achieve better insight into the molecular structure of the most preferentially tautomeric ligand forms and complexes, the conformational analysis of the studied compounds were performed. This was carried out by use of MM+ force field [32,33] using Hyperchem. 7.5 program [34], (calculations in vacuo, bond dipole option for electrostatics, Polak–Ribiere algorithm, RMS gradient of 0.1 kcal/Å mol). Furthermore, the geometrical optimization with semi-empirical (PM3) molecular orbital method was preformed [35]. The computed molecular parameters, total energy, binding energy, heat of formation, the lowest unoccupied molecular orbital (LUMO) and the highest occupied molecular orbital (HOMO) energies, and the dipole moment for studied compounds were calculated (Table 2). It is obvious that there is a possibility of existence the prepared ligand in both keto–enol forms. Moreover, the experimental determination of the tautomeric ligand structure is complicated and often unpredictable. The calculated molecular parameters have been used to investigate the most stable isomer of the keto–enol forms of the prepared ligand (βAS) and showed that the most stable tautomer is the keto form (Fig. 6). The conjugation of the π-electrons of the carbonyl groups with the π-system of the molecular skeleton probably reduces the energy of the keto form, which leads to its predominance over the enol one.

The total energy, binding energy, heat of formation, LUMO and HOMO energies were also, calculated for the copper(II) complex (Table 2) and indicated that the Cu^{II}βAS in the keto form is more stable even when compared to the two ligand isomers. The bond length between carbon and oxygen in CO in case of the keto form of Cu^{II}βAS was found to be shorter than that in case of COH in enol form. The bond length and bond angle for the keto–enol forms of the

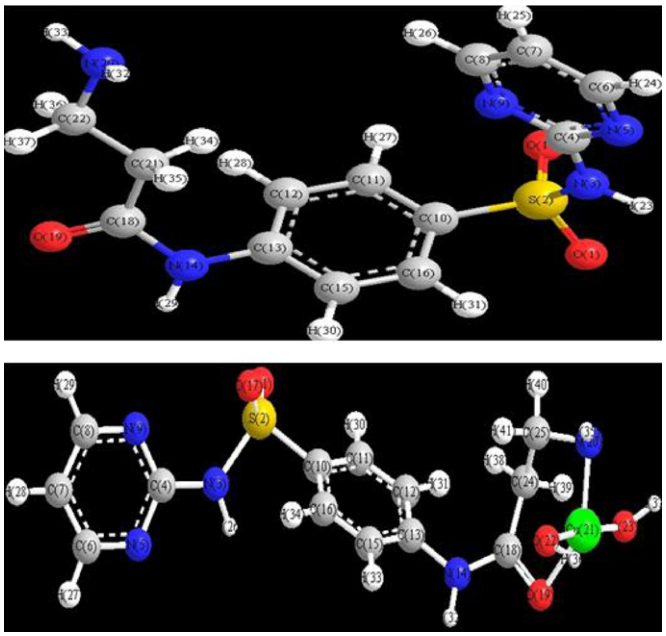

Fig. 6. Ball and stick rendering for the most stable tautomer form of the ligand (keto form of βAS) and complex (from above to below, respectively), as calculated by PM3 semi-empirical molecular orbital calculations.

ligand together with the most stable complex isomer are calculated and listed in Tables S1 and S2 (supplementary data).

4. Oxidation of trihydroxybenzene

Since environmental and economic factors make the use of harmful oxidants increasingly unacceptable except on a small scale, hydrogen peroxide is used in the oxidation of polyphenol 1,2,3-trihydroxybenzene (THB). In this study the Cu^{II}—βAS complex was used to activate the green oxidant H_2O_2 in the oxidation of THB affording an effective catalyst.

In order to study the catalytic activity of the Cu^{II}—βAS and its interaction with H_2O_2 toward the oxidation of 1,2,3-trihydroxybenzene, THB has been used as a substrate to provide detailed kinetic information. The oxidation rates of THB by 30 μM Cu^{II}—βAS at different concentrations of THB (Fig. 7) were determined in the presence of 200 μM H_2O_2. The rate of THB oxidation is found to be nonlinear, reaching saturation at high THB

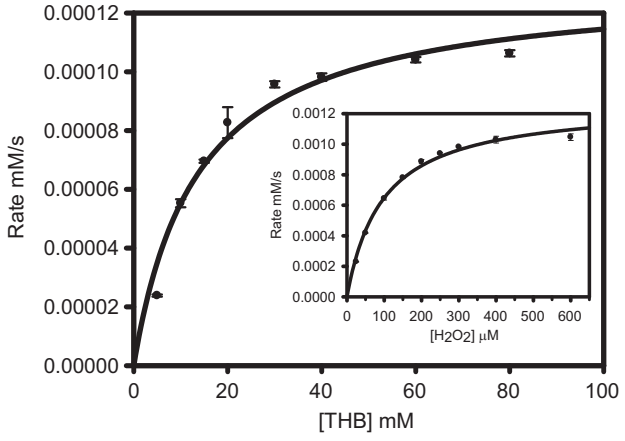

Fig. 7. Oxidation of THB using 30 μM of Cu^{II}—βAS in the presence of 200 μM H_2O_2 at 25 °C. Inset shows the oxidation of 30 mM THB in the presence of different concentration of H_2O_2.

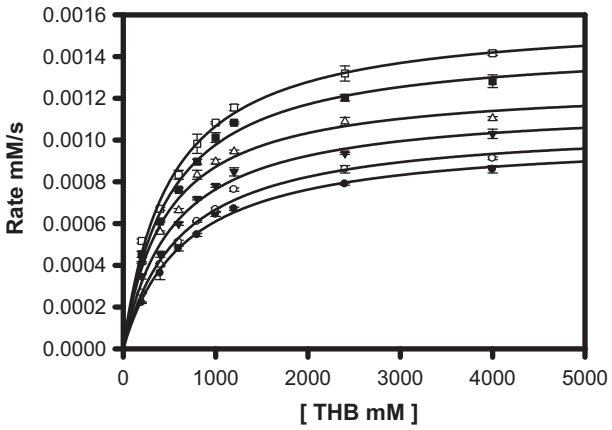

Fig. 8. Oxidation of THB at 50 μM H_2O_2 (●), 100 μM H_2O_2 (○), 150 μM H_2O_2 (▼), 200 μM H_2O_2 (△), 250 μM H_2O_2 (■), 300 μM H_2O_2 (□) using 40 μM Cu^{II}—βAS at 25 °C.

concentrations which suggest an enzyme-like pre-equilibrium kinetics. This kinetics can be described as the binding of THB with the catalyst Cu^{II}—βAS to form an intermediate THB—Cu^{II}—βAS complex, followed by conversion of the bound substrate (THB) into products (Eq. (5)). The rate law for this reaction can be obtained with steady-state approximation similar to the Michaelis–Menten kinetics in enzyme catalysis. The rate law for this reaction mechanism can be expressed as in Eq. (6), wherein $K' = (k_{-1} + k_{cat})/k_1$ is the dissociation constant of the THB—Cu^{II}—βAS complex. The reaction in the presence of saturation amount of H_2O_2 (200 μM) produces a first-order rate constant $k_{cat} = 0.0043\ s^{-1}$ ($t_{1/2} = 161$ s) and dissociation constant $K' = 13.5$ mM. The Cu^{II}—βAS affords a significant catalytic efficiency $k_{cat}/K' = 0.32\ M^{-1}\ s^{-1}$ as the second order rate constant. The catalysis shows 1.7×10^3 times rate enhancement in terms of the first-order rate constant (k_{cat}/k_o, wherein $k_o = 2.53 \times 10^{-6}\ s^{-1}$ is the rate constant for the uncatalyzed reaction "oxidation of 30 mM THB with 200 μM H_2O_2 under the same reaction conditions").

The oxidation of the trihydroxybenzene as a function of H_2O_2 also shows a saturation pattern at high concentrations (Fig. 7, inset), indicating direct binding of this oxidant to the active metal center. Therefore, both THB and H_2O_2 are considered to be substrates. For a bi-substrate binding mechanism, the binding of two substrates (THB and H_2O_2) to the active center of Cu^{II}—βAS can be described in terms of the Hanes equation (Eq. (7)) [36].

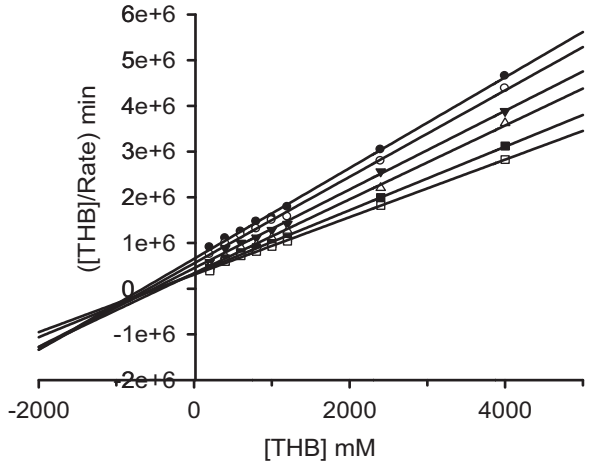

Fig. 9. Hanes plot of oxidation of THB using 40 μM Cu^{II}—βAS in the presence of 50, 100, 150, 200, 250 and 300 μM H_2O_2 (from top).

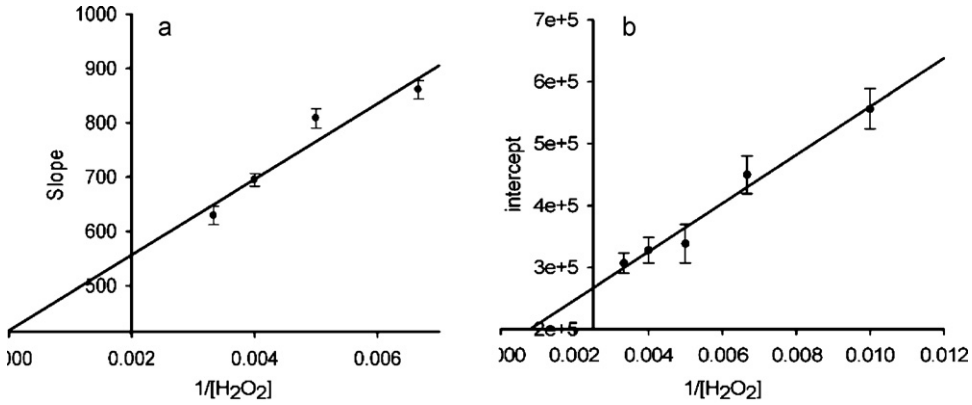

Fig. 10. (a) Replotting the slope obtained from Fig. 9 versus $1/[H_2O_2]$; (b) repotting the *y*-intercept obtained from Fig. 9 versus $1/[H_2O_2]$.

Hanes analysis was used to calculate the apparent and intrinsic dissociation constants (Fig. 8). It is important to determine the rates at varying amounts of H_2O_2 with a fixed concentration of THB and vice versa. Fig. 10a and b shows the conversion of the plot in Fig. 9 to a secondary plot of the slope ($1/V_{max}$) and *y*-intercept (K_{app}/V_{max}) as a function of $1/[H_2O_2]$, affording $K'_{(THB)} = 404.39$ mM, $K_{i(THB)} = 560.88$ mM, $K'_{(H_2O_2)} = 62.30$ mM and $K_{i(H_2O_2)} = 122.05$ mM. The K'/K_i ratio is 0.72 for THB and 0.51 for H_2O_2 which indicates that the binding of these two substrates are not equally exclusive. At the same time it shows the presence of a small cooperativity [37] among Cu^{II} centers for polyphenol oxidation by Cu^{II}—βAS. This cooperativity may be results from dinuclear catalysis of the 2-electron oxidation of polyphenol. Cooperativity is a phenomenon displayed by enzymes or receptors that have multiple binding sites. When a substrate binds to one enzymatic subunit, the rest of the subunits are stimulated and become active (positive cooperative binding). To investigate the existence of free radical in the reaction mechanism, various concentrations of $(CH_3)_2SO$ have been used in the oxidation of 1.0 mM THB in the presence of H_2O_2 using Cu^{II}—βAS. The free radical scavenger $(CH_3)_2SO$ [38] did not inhibit the reaction under the experimental conditions, suggesting the absence of free radical to induce the oxidation reaction (Fig. 11).

Because the oxidation of catechols is a two-electron transfer process, the involvement of a dinuclear copper center is thus a preferred pathway as in the case of the enzyme [39,40]. Based on the kinetic data described in this study and according to the catalytic pathways of catechol oxidase, a random bi-substrate mechanism is proposed (Fig. 12). In the absence of the green oxidant H_2O_2, THB is bound to and oxidized by Cu^{II}—βAS complex in form of a dinuclear Cu^{II}-center by inner-sphere 2-electron transfer to yield Cu^{I}_2 and *o*-quinone product (steps **A** and **B**). The dinuclear center can be formed from two Cu^{II} centers on two different copper

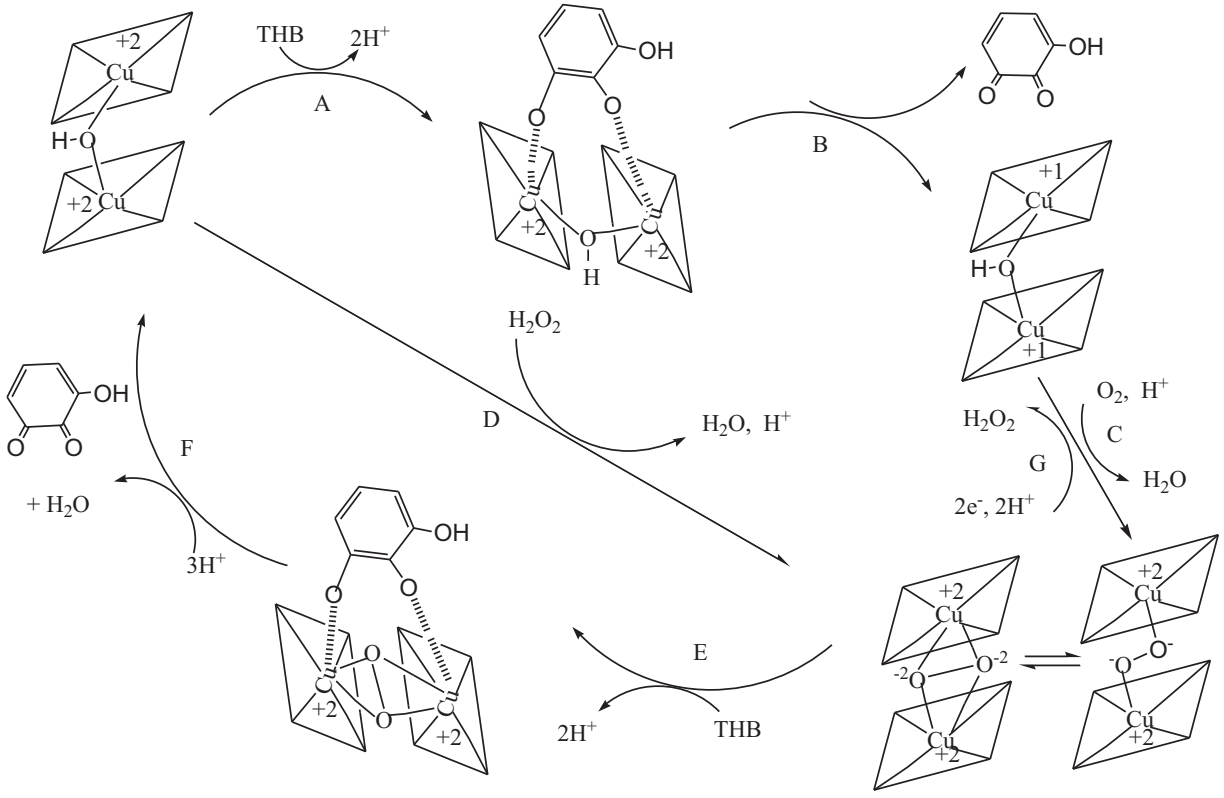

Fig. 11. Proposed mechanism for the oxidation of THB by Cu^{II}—βAS in the absence (**A**–**C** and E–F) and presence (steps D–F) of H_2O_2.

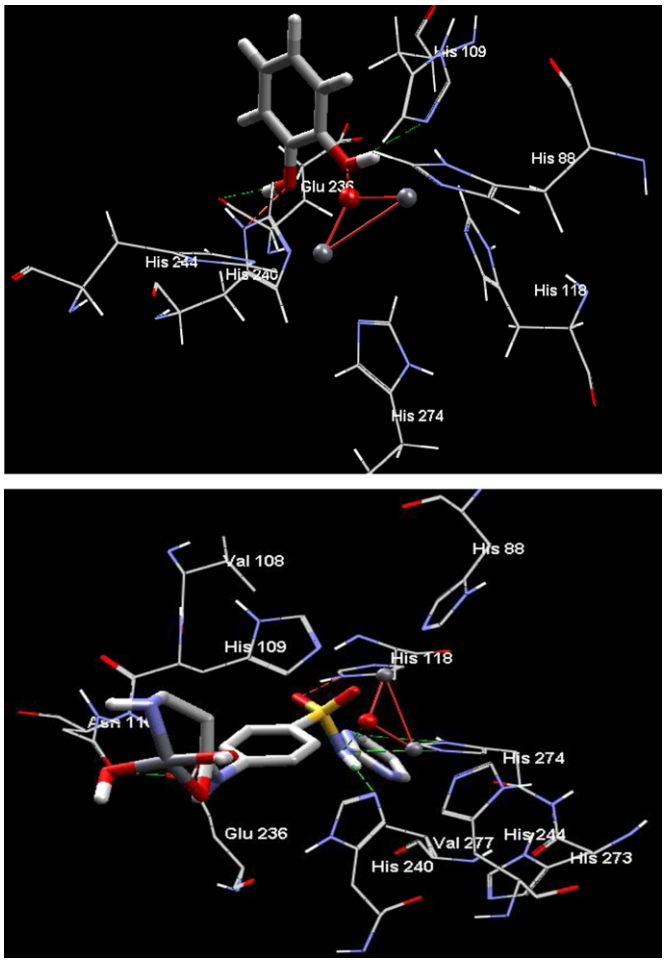

Fig. 12. Docking of catechol (stick mode) to the dinuclear Cu^{II} site reveals a favorable binding configuration, *green dot lines represented* H-bonding with the bridging peroxide site, *red dot lines represented* electrostatic bonding with the bridging peroxide site. Docking of Cu^{II}—βAS (stick mode) to the dinuclear Cu^{II} site reveals a favorable binding configuration, *green dot lines represented* H-bonding with the bridging peroxide site, *red dot lines represented* electrostatic bonding with the bridging peroxide site. (For interpretation of the references to color in this figure legend, the reader is referred to the web version of the article.)

complexes [15,41]. The inner-sphere electron transfer is followed by dioxygen binding (**C**) (whereas the molecular oxygen serves as a second substrate in this case) to form a dinuclear Cu^{II}-peroxo center or its isoelectronic form [14,16] which can also be formed upon peroxide binding (D). In the presence of THB and H_2O_2, the dinuclear μ-η^2:η^2-peroxo-Cu_2^{II}-THB transition state is eventually formed by assembling two metal centers together via the bridging peroxo (steps D and E) as in the case of many mononuclear Cu^{II}-complexes [42,43]. Formation of the transition state is followed by 2-electron transfer from the bound catechol to the bound peroxide (likely through the metal center) to yield Cu_2^{II}-μ-OH and *o*-quinone to complete a catalytic cycle (step F). Under the reduction conditions the Cu^{II}-peroxo intermediate is expected to undergo through the pathway G to produce H_2O_2.

Molecular mechanical calculations have been applied to determine the structure of Cu^{II}—βAS binding mode using (MOE version 2007). The kinetic studies results are in agreement with a dinuclear catalysis model, the active oxygenated intermediate is modeled with a dinuclear center analogous to that of hemocyanin with a pseudo-C_{2h} symmetry [44,45]. This oxy/peroxy dinuclear site allows substrate binding to one of the metal ions from the top or bottom of the Cu—O_2—Cu plane without distorting the overall coordination sphere. A catechol substrate can be docked into

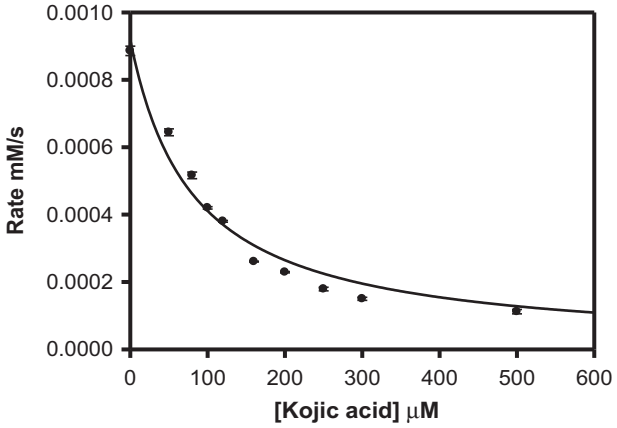

Fig. 13. Inhibition toward oxidation of THB using 40 μM Cu^{II}—βAS by kojic acid in the presence of 200 μM H_2O_2.

the dinuclear site of peroxide-bound Cu^{II}—βAS without significant distortion (Fig. 12a), in which the first hydroxy group of catechol is bound to O center with an electrostatic bond and bound to His^{109} with H-bond, while the second hydroxy group of catechol forms a H-bond with Glu^{236} and electrostatic bond with His^{240} with energy (−450 kcal/mol). Also, Cu^{II}—βAS forms H-bond with (Asn^{119}, His^{240} and His^{274}) through (Cu atom, nitrogen atom of $NHSO_2$ and O atom of OSO) respectively (Fig. 12b), with lowest energy (−570.12 kcal/mol).

In order to investigate the effect of the catalyst concentration on the oxidation of THB with 200 μM H_2O_2, different concentrations of the copper complex Cu^{II}—βAS have been used in the oxidation of 1.0 mM THB. The observed rate was found to be linear till 50 μM of copper complex and then reaches saturation indicating that the optimum concentration for the copper complex should be around 50 μM.

Inhibition of trihdyroxybenzene oxidation by kojic acid. Since kojic acid is a well known compound for inhibition of polyphenol oxidation by oxidases [46]. It was used to inhibit Cu^{II}—βAS complex toward oxidation of trihydroxybenzene. Fig. 13 shows that the kojic acid significantly inhibits the oxidation of THB with $IC_{50} \sim 65$ μM.

5. Conclusion

The organic ligand β-alanylsulfadiazine (βAS) was prepared by reacting sulfadiazine with β-alanine amino acid. The ligand was fully characterized by different techniques. The conformational analysis showed that the keto form of βAS is more stable than the enol one. The simple copper(II) complex of β-alanylsulfadiazine was fully characterized by means of IR, UV/Vis, elemental analysis, EPR and thermal analysis. The geometry around the copper ion is found to be square planar and the average diameter of the complex is found to be in the range of 35–40 nm. The Cu^{II}—βAS complex has been used as a catalyst in the oxidation of polyphenol 1,2,3-trihydroxybenzene in the presence of H_2O_2 as a green oxidant. Cu^{II}—βAS affords a significant catalytic activity toward the oxidation of THB compared to the uncatalyzed reaction. The oxidation reaction mechanism proposed in this study demonstrated two-electron transfer process involving dinuclear copper center as in case of catechol oxidase. The oxidation reaction herein is inhibited by kojic acid.

Acknowledgment

The authors acknowledge Taif University for supporting this work by Taif University research program (1-430-473).

Appendix A. Supplementary data

Supplementary data associated with this article can be found, in the online version, at doi:10.1016/j.molcata.2011.12.016.

References

[1] J. Haggin, Chem. Eng. News 71 (1993) 23–27.
[2] L.I. Simándi, Catalytic Activation of Dioxygen by Metal Complexes, Kluwer, Dordrecht, 1992.
[3] R. Than, A.A. Feldman, B. Krebs, Coord. Chem. Rev. 182 (1999) 211–241.
[4] F. Zippel, F. Ahlers, R. Werner, W. Haase, H.F. Nolting, B. Krebs, Inorg. Chem. 35 (1996) 3409–3419.
[5] J. Reim, R. Werner, W. Haase, B. Krebs, Chem. Eur. J. 4 (1998) 289–298.
[6] B. Srinivas, N. Arulsamy, P.S. Zacharias, Polyhedron 10 (1991) 731–736.
[7] M.R. Malachowski, M.G. Davidson, Inorg. Chim. Acta 162 (1989) 199–204.
[8] K.D. Karlin, Y. Gultneh, T. Nicholson, J. Zubieta, Inorg. Chem. 24 (1985) 3725–3727.
[9] M.R. Malachowski, M.G. Davidson, J.N. Hoffman, Inorg. Chim. Acta 157 (1989) 91–94.
[10] E.V. Rybak-Akimova, D.H. Busch, P.K. Kahol, N. Pinto, N.W. Alcock, H.J. Clase, Inorg. Chem. 36 (1997) 510–520.
[11] J.F. Larrow, E.N. Jacobsen, Y. Gao, Y.P. Hong, X.Y. Nie, C.M. Zepp, J. Org. Chem. 59 (1994) 1939–1942.
[12] T. Punniyamurth, S. Velusamy, J. Igbal, Chem. Rev. 105 (2005) 2329–2364.
[13] H. Okawa, H. Sakiyama, Pure Appl. Chem. 67 (1995) 273–280.
[14] L.Q. Hatcher, K.D. Karlin, J. Biol. Inorg. Chem. 9 (2004) 669–683.
[15] E.A. Lewis, W.B. Tolman, Chem. Rev. 104 (2004) 1047–1076.
[16] N. Kitajima, Y. Moro-oka, Chem. Rev. 94 (1994) 737–757.
[17] V. Lykourinou, A.I. Hanafy, G.F.Z. da Silva, K.S. Bisht, R.W. Larsen, B.T. Livingston, A. Angerhofer, L.J. Ming, Eur. J. Inorg. Chem. (2008) 2584–2592.
[18] E. Wünsch, E. Jaeger, L. Kisfaludy, M. Löw, Angew. Chem. 16 (1977) 317–318.
[19] H.Y. Mostafa, J. Pigment Resin. Res. Technol. 35 (2006) 71–75.
[20] P. Selvam, P. Rathore, S. Karthikumar, K. Velkumar, P. Palanisamy, S. Vijayalakhsmi, M. Witvrouw, Ind. J. Pharm. Sci. 71 (2009) 432–436.
[21] T. Ahamad, N. Nishat, J. Appl. Polym. Sci. 107 (2008) 2280–2288.
[22] J. Ribas, C. Diaz, R. Costa, Y. Journauv, C. Mathoniere, O. Kahn, A. Gleizes, Inorg. Chem. 29 (1990) 2042–2047.
[23] C. Fraser, B. Bosnich, Inorg. Chem. 33 (1994) 338–346.
[24] T. Ahamad, V. Kumar, S. Parveen, N. Nishat, J. Coord. Chem. 61 (2008) 47–56.
[25] N. Nishat, T. Ahamad, S.M. Alshehri, S. Parveen, Eur. J. Med. Chem. 45 (2010) 1287–1294.
[26] R.J. Dudley, B.J. Hathaway, J. Chem. Soc. (1970) 1725–1728.
[27] B.J. Hathaway, D.E. Billing, Coord. Chem. Rev. 5 (1970) 143–207.
[28] A.W. Coats, J.P. Redfern, Nature 201 (1964) 68–69.
[29] F. Yakuphanoglu, A.O. Gorgulu, A. Cukurovali, Physica B 353 (2004) 223–229.
[30] A.M. Yu, Z.J. Liang, J.H. Cho, F. Caruso, Nano Lett. 3 (2003) 1203–1207.
[31] Y. Xiao, F. Patolsky, E. Katz, J.F. Hainfeld, I. Willner, Science 299 (2003) 1877–1881.
[32] S. Profeta, N.L. Allinger, J. Am. Chem. Soc. 107 (1985) 1907–1918.
[33] N.L. Allinger, J. Am. Chem. Soc. 99 (1977) 8127–8134.
[34] HyperChem. Version 7.51, Hypercube Inc., FL, USA, 2003.
[35] J.J.P. Stewart, Applicat. J. Comput. Chem. 10 (1989) 221–264.
[36] Leskovac, Comperhensive Enzyme Kinetics, Kluwer/Plenum, Boston, 2002, p. 119.
[37] J.R. Florini, C.S. Vestling, Biochem. Biophys. Acta 25 (1957) 575–578.
[38] P.S. Rao, J.M. Luber, J. Milinowicz, P. Lalezari, H.S. Mueller, Biochem. Biophys. Res. Commun. 150 (1988) 39–44.
[39] E.I. Solomon, U.M. Sundaram, T.E. Machonkin, Chem. Rev. 96 (1996) 2563–2605.
[40] C. Gerdemann, C. Eicken, B. Krebs, Acc. Chem. Res. 35 (2002) 183–191.
[41] W.B. Tolman, Acc. Chem. Res. 30 (1997) 227–237.
[42] N. Kitajima, T. Koda, Y. Iwata, Y. Morooka, J. Am. Chem. Soc. 112 (1990) 8833–8839.
[43] W.B. Tolman, Acc. Chem. Res. 30 (1997) 227–230.
[44] B. Hazes, K.A. Magnus, C. Bonaventura, J. Bonaventura, Z. Dauter, K.H. Kalk, W.G.J. Hol, Protein Sci. 2 (1993) 597–619.
[45] K.A. Magnus, B. Hazes, H. Tonthat, C. Bonaventura, J. Bonaventura, W.G.J. Hol, Proteins – Struct. Funct. Genet. 19 (1994) 302–309.
[46] G. Battaini, E. Monzani, L. Casella, L. Santagostini, R. Pagliarin, J. Biol. Inorg. Chem. 5 (2000) 262–268.